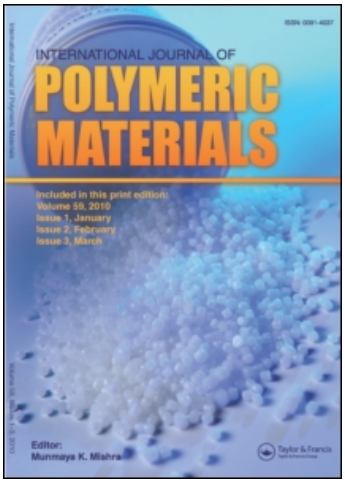

International Journal of Polymeric Materials
Publication details, including instructions for authors and subscription information:
http://www.informaworld.com/smpp/title~content=t713647664

Young's Modulus Estimated from Orientation Distribution Functions of Crystal and Amorphous Phases for Simultaneous Biaxially Stretching Ultra-High Molecular Weight Polyethylene Films Prepared by Gelation/Crystallization from Solutions

Teruo Nakashima[a]; Chunye Xu[b]; Yuezhen Bin[b]; Masaru Matsuo[b]
[a] Toyooka Junior College, Kinki University, Toyooka, Japan [b] Department of Textile and Apparel Science, Faculty of Human Life and Environment, Nara Women's University, Nara, Japan

Online publication date: 27 October 2010

To cite this Article Nakashima, Teruo , Xu, Chunye , Bin, Yuezhen and Matsuo, Masaru(2002) 'Young's Modulus Estimated from Orientation Distribution Functions of Crystal and Amorphous Phases for Simultaneous Biaxially Stretching Ultra-High Molecular Weight Polyethylene Films Prepared by Gelation/Crystallization from Solutions', International Journal of Polymeric Materials, 51: 1, 77 — 102
To link to this Article: DOI: 10.1080/00914030213034
URL: http://dx.doi.org/10.1080/00914030213034

International Journal of Polymeric Materials, 51:77–102, 2002

0091-4037/02 $12.00+.00

Young's Modulus Estimated from Orientation Distribution Functions of Crystal and Amorphous Phases for Simultaneous Biaxially Stretching Ultra-High Molecular Weight Polyethylene Films Prepared by Gelation/Crystallization from Solutions

TERUO NAKASHIMA [a], CHUNYE XU [b], YUEZHEN BIN [b] and MASARU MATSUO [b,*]

[a]*Kinki University of Toyooka Junior College, Toyooka 160 Japan;*
[b]*Department of Textile and Apparel Science, Faculty of Human Life and Environment, Nara Women's University, Nara 630 Japan*

(Received 21 December 2000; In final form 8 January 2001)

Young's modulus of simultaneous biaxially stretched films was much lower than that of uniaxial films with the same draw ratio. To address this problem, a theoretical approach was carried out by using a three-dimensional model. In this model system, the oriented crystalline layers are surrounded by an anisotropic amorphous phase and the strains of the two phases at the boundary are identical. Young's modulus was calculated by using the generalized orientation factors of crystallites and amorphous chain segments calculated from the orientation function of crystallites and that of amorphous chain segments. The orientation function of crystallites was determined from the orientation functions of the reciprocal lattice vectors of the crystal planes. The theoretical values of Young's modulus were calculated using the values of elastic compliance proposed by Zehnder. The values were in fairly good agreement with the experimental values of specimens with different draw ratios. Judging from the induced equations, the calculated results provided that the Young's modulus of simultaneous biaxially stretching film is

*Corresponding author.

attributed to the contribution from the compliance associated with shear modulus and consequently the Young's modulus automatically takes low values.

Keywords: Ultrahigh M; Polyethylene; Films; Young Modulus; Orientation distribution functions

INTRODUCTION

The biaxial drawing of UHMWPE was first done by Sakai *et al.* [1–3]. They studied the development of fibrillar texture and mechanical properties of UHMWPE dry gel films. Further considerations of the deformation mechanism and mechanical properties have been published by Gerrits *et al.* [4–6] and Bastiannsen *et al.* [7] in terms of experimental and theoretical aspects. They pointed out that Young's modulus and the tensile strength are not improved in contrast to those of uniaxially drawn tapes. A detailed analysis of the deformation mechanism was discussed in terms of crystal plasticity on the basis of the planar orientation of the crystal planes. Among their reports [4–9], a detailed analysis was done by Gerrits and Young [6]. They analyzed the crystal orientation in terms of crystal plasticity associated with both slip and twinning processes and hexagonal and martensitic phase transformations by using 10 times biaxially drawn films.

To give a more quantitative treatment of simultaneous biaxially stretching mechanism of UHMWPE dry gel films, this paper deals with the estimation of Young's modulus of the films in relation to the optimum concentration assuring the greatest significant drawability of UHMWPE. In a previous paper [8], the deformation mechanism was analyzed using the orientation distribution function of crystallites which can be determined from uniaxial orientation distribution functions of the reciprocal lattice vectors of the crystal planes around the film normal direction in accordance with the method of Roe and Krigbaum [9–11]. Furthermore, the ultimate values of simultaneous biaxially oriented polyethylene films was estimated as ideal cases with 100% crystallinity as well as the perfect orientation of the c-axes parallel to the film surface. The function of the reciprocal lattice vectors of the crystal planes has never been reported for a very thin film with thickness less than 10 mμ because

of the difficulty in piling up a number of thin sheets. Much effort was invested in the development of a small but refined instrument to stack a number of thin sheets. In this paper, as a real system to compare the experimental results with theoretical ones, more complicated calculation for the Young's modulus was carried out by using a three-dimensional model. In this model system [12], the oriented crystalline layers are surrounded by an anisotropic amorphous phase and the strains of the two phases at the boundary are identical. Young's modulus was calculated by using the generalized orientation factors of crystallites and amorphous chain segments calculated from the orientation functions of crystallites and amorphous chain segments. The mathematical treatment in this paper is much more complicated in comparison with that in the previous paper [8]. Of course, the present treatment is quite different from the method proposed by Sakai *et al.* [2]. There are problems in their treatment, since the Young's modulus obtained by them corresponds only to the value along the direction perpendicular to the c-axis within a polyethylene crystal unit cell. In their treatment, no orientational effect of the c-axes was considered. Accordingly, the calculation was carried out as a function of the tilting angle from the c-axis.

EXPERIMENTAL SECTION

Sample Preparation

As described in the previous paper [8], the samples used in this experiment were UHMWPE (Hercules 1900/90189) with a viscosity-average molecular weight ($\overline{M}_v$) of 6×10^6. The solvent was decalin. The concentrations of UHMWPE chosen were 0.4, 0.6, 0.7, 0.8, 0.9, 1.0 g/100 ml. Decalin solutions were prepared by heating the well-blended polymer-solvent mixture at 135°C for 40 min under nitrogen. The solution was stabilized with 3% w/w of antioxidant (di-t-butyl-p-cresol) against UHMWPE. The hot homogenized solution was quenched to room temperature by pouring it into an aluminum tray, thus generating a gel. The decalin was allowed to evaporate from the gels under ambient conditions. The resulting dry

gel film was vacuum-dried for 1 day to remove residual trace of decalin.

The dry gel film was cut into strips of 90×90 mm. The specimens were held at 150°C for 5 min and elongated biaxially to the desired ratio using an Iwamoto biaxial stretcher. The draw ratio was determined in the usual way by measuring the displacement of ink marks placed 5×5 mm apart on the specimen prior to drawing. Immediately after stretching, the sample fixed in the stretcher was quenched to room temperature. Unlike the case of uniaxial elongation, no necking occurred under simultaneous biaxially stretching.

Crystallinity was calculated assuming intrinsic densities of crystalline and amorphous phases to be 1.000 and 0.852 g/cm^3 respectively [13]. These results were reported already in the previous paper [8].

Table I(a) shows Young's modulus and tensile strength at the maximum draw ratio of the films prepared by gelation/crystallization from solutions with the indicated concentrations > 0.7 g/100 ml. The data reported elasewhere [8] are shown in this paper again, since the experimental results are very important to discuss the mechanical properties in comparison with the theoretical results discussed later. Young's modulus becomes higher and the maximum value occured at 1.0 g/100 ml with increasing concentration. Interestingly, the Young's modulus and tensile strength of the films (7.8×7.8) prepared from a 1.0 g/100 ml solution are higher than those of the film (8.7×8.7) prepared from a 0.9 g/100 ml solution. This indicates that Young's modulus is sensitive to the number of entanglements within the specimen, when the orientation of the c-axes increases to a certain degree. Namely, Young's modulus increases with increased number of

TABLE I(a) Young's modulus and tensile strength of simultaneous biaxial stretching films; Young's modulus and tensile strength at the maximum draw ratio of the specimens prepared from the solutions with the indicated concentrations

Maximum draw ratio (λ_{max})	*Concentration* ($g/100\,ml$)	*Young's modulus* (GPa)	*Tensile strength* (GPa)
7.3×7.3	0.7	2.5	0.12
7.7×7.7	0.8	3.5	0.14
8.7×8.7	0.9	4.3	0.16
7.8×7.8	1.0	4.4	0.19

TABLE I(b) Young's modulus and tensil Strength of simultaneous biaxial stretching films; Young's modulus and tensile strength as a function of concentration of solutions to prepare gels

Draw ratio (λ)	*Concentration* ($g/100\,ml$)	*Young's modulus* (GPa)	*Tensile strength* (GPa)
	0.4	1.8	0.05
	0.6	1.9	0.07
2.0×2.0	0.7	2.0	0.08
	0.8	2.1	0.09
	0.9	2.2	0.10
	1.0	2.3	0.11
	0.6	1.9	0.09
	0.7	2.2	0.10
6.0×6.0	0.8	3.2	0.12
	0.9	3.6	0.13
	1.0	3.9	0.14

entanglements. Table I(b) shows the concentration dependence of Young's modulus and tensile strength at 2×2 and 6×6. The results indicate that even for the specimens with draw ratio 2×2, Young's modulus and tensile strength are more pronounced with increasing concentration. This result supports the importance of the number of entanglements within the drawn film in Table I(a) to improve mechanical properties.

As listed in Table I(a), an apparent problem is that Young's modulus and tensile strength, even for the films with draw ratio $> 7 \times 7$ ($= 49$), are less than 4.5 GPa and 0.2 GPa, respectively, while the Young's modulus and tensile strength corresponding to uniaxial films with a draw ratio of 50 times were $25 - 30$ GPa and $0.8 - 1$ GPa, respectively [14]. Even so, the values of the Young's modulus and tensile strength of simultaneous biaxially stretched films are higher than the corresponding values of 0.1 GPa and 0.08 GPa of the commercial blown films (crystallinity 52%, melting point 138°C).

Experimental Procedures of X-ray Diffraction Measurements

The X-ray measurements were carried out with a 12 kW rotating-anode X-ray generator (Rigaku RDA-rA) operated at 200 mA and

40 kV. The intensity curve $I_{cry}(2\theta_B)$ as a function of twice of the Bragg angle $2\theta_B$ was separated into the contribution from the individual crystal planes, assuming that each peak had a symmetric form given by a Lorenzian function of in Eq. (1), where I_j^o is the maximum intensity of the j-th peak.

$$I_{cry}(2\theta_B) = \sum_j \frac{I_j^o}{1 + (2\theta_o^j - 2\theta_B)^2/\beta_j^2} \tag{1}$$

Here β_j is the half-width of the j-th peak at half of the peak intensity and θ_o^j is the Bragg angle at which the maximum intensity of the j-th peak appears. Using the same process at a given θ_j in the range from 0 to 90°, the intensity distribution I_j $(2\theta_B)$ can be determined for the respective j-th plane after integrating $I_{cry}(2\theta_B)$ by $2\theta_B$ at each θ_j, and consequently the orientation distribution function $2\pi q_j(\cos\theta_j)$ of the j-th reciprocal lattice vector may be given by

$$2\pi q_j(\cos\theta_j) = \frac{I_j(\theta_j)}{\int_0^{\pi/2} I_j(\cos\theta_j)\sin\theta_j d\theta_j} \tag{2}$$

Orientation Distribution Function of the Reciprocal Lattice Vectors of the Crystal Planes

Figure 1(a) shows Cartesian coordinate $0-U_1U_2U_3$ fixed within a structural unit, with respect to another Cartesian coordinate $0-X_1X_2X_3$ fixed in a bulk specimen. The U_3 axis may be taken along the c-axis. Because of the simultaneous biaxially stretched film, the c-axes have a random orientation around the X_3 axis (the film thickness direction) in the present system. The orientation of the structural unit within the space of the film specimen may be specified by using three Euler angles, ϕ, θ, and η. The angles θ and ϕ, which define the orientation of the U_3 axis of the unit within the space, are polar and azimuthal angles, respectively, and η specifies the rotation of the unit around its own U_3 axis. Coordinates (b) and (c) show a given j-th axis r_j within the unit, specified by the polar angle θ_j and the azimuthal angle ϕ_j with respect to the Cartesian coordinate $0-X_1X_2X_3$ and

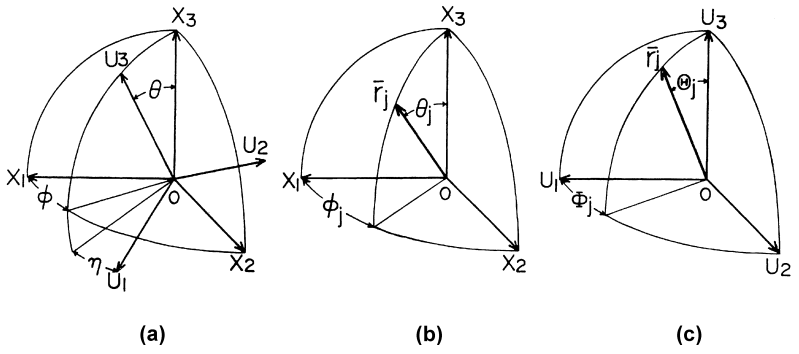

FIGURE 1 Cartesian coordinate illustrating the geometrical relation (a) Euler angles θ and η which specify the orientation of coordinate $0-U_1U_2U_3$ of structural unit with respect to coordinate $0-X_1X_2X_3$ of specimen. (b) Angles θ_j and ϕ_j which specify the orientation of the given j-th axis of the structural unit with respect to the coordinate $0-X_1X_2X_3$. (c) Angles Θ_j and Φ_j which specify the orientation of the j-th axis of the structural unit with respect to the coordinate $0-U_1U_2U_3$.

specified by polar angle Θ_j and the azimuthal angle Φ_j with respect to the $0-U_1U_2U_3$ of the unit.

For an uniaxially system, the orientation distribution function $\omega(\cos\theta, \eta)$ of crystallites may be calculated from the orientation distribution function of the reciprocal lattice vector of the j-th plane, $2\pi q(\cos\theta_j)$, by using a method proposed by Roe and Krigbaum [9–11].

$$F^j_{\ell 0} = \langle P_\ell(cos\,\theta_j)\rangle = \int_0^{2\pi}\int_0^{\pi} q_j(cos\,\theta_j)P_\ell(cos\,\theta_j)sin\,\theta_j d\theta_j d\phi_j \qquad (3)$$

$$F^j_{\ell 0} = F_{\ell 00}P_\ell(cos\,\Theta_j) + 2\sum_{n=2}^{t}\frac{(\ell-n)!}{(\ell+n)!}F_{\ell 0n}P^n_\ell(cos\,\Theta_j)cos\,n\Phi_j \qquad (4)$$

$$4\pi^2\omega(\cos\theta,\eta) = \frac{1}{2} + \sum_{\ell=2}^{\infty}\frac{(2\ell+1)}{2}\left\{F_{\ell 00}P_\ell(\cos\theta) + 2\sum_{n=2}^{\ell}\frac{(\ell-n)!}{(\ell+n)!}F_{\ell 0n}\cos n\eta\right\} \qquad (5)$$

Here ℓ and n are even integers. $P_\ell^n(X)$ and $P_\ell(X)$ are the associated Legendre polynomials and Legendre polynomials, respectively. $F_{\ell 0}^j$ and $F_{\ell 0n}$ are the coefficients. $F_{\ell 0}^j$ is the ℓ-th order orientation factor of the j-th crystal plane estimated by X-ray diffraction, while the generalized orientation factor $F_{\ell 0n}$ can be determined by solving the linear equations represented by Eq. (4), since there exist more equations than the number of unknowns, as was pointed out by Roe and Krigbaum [9–11].

The values of weighing factors ρ_j, required in the least-squares calculation, were assigned somewhat subjectively on the assumption that the X-ray diffraction intensity is dependent upon the structure factor of each crystal plane. Hence, in this calculation, the weighing factors ρ_j, as a first approximation, were assumed to be almost proportional to the structure factor and were subsequently modified to obtain the best fit between experimental and calculated results through numerical calculations by computer. The calculation was continued until the best fit was achieved within the capability of the simplex method [15]. Using the final values of parameters, a mean-square error between the calculated $F_{\ell 0}^j$ and recalculated $F_{\ell 0}^j$ was obtained using:

$$R = \frac{\sum_j \sum_\ell \rho_j \left[(F_{\ell 0}^j)_{cal} - (F_{\ell 0}^j)_{recal} \right]^2}{\sum_j \sum_\ell \left[(F_{\ell 0}^j)_{cal} \right]^2} \tag{6}$$

Figures 2 ~ 4 compare the observed orientation distribution functions $2\pi q_j(\cos\theta_j)$ with those recalculated for the respective crystal planes for the films with $\lambda = 1 \times 1$ (the undrawn film), 2×2, and 8.7×8.7, respectively, which were prepared from a 0.9 g/100 ml solution. We calculated $F_{\ell 0}^j$ from Eq. (4) to minimize the value of R in Eq. (6). After that, we recalculated $F_{\ell 0}^j$, in turn, from the values of $F_{\ell 0n}$, and further calculated $2\pi q_j(\cos\theta_j)$ from the recalculated $F_{\ell 0}^j$ value using the following equation:

$$2\pi q_j(\cos\theta_j) = \frac{1}{2} + \sum_{\ell=2}^{\infty} \frac{2\ell+1}{2} F_{\ell 0}^j P_\ell(\cos\theta_j) \tag{7}$$

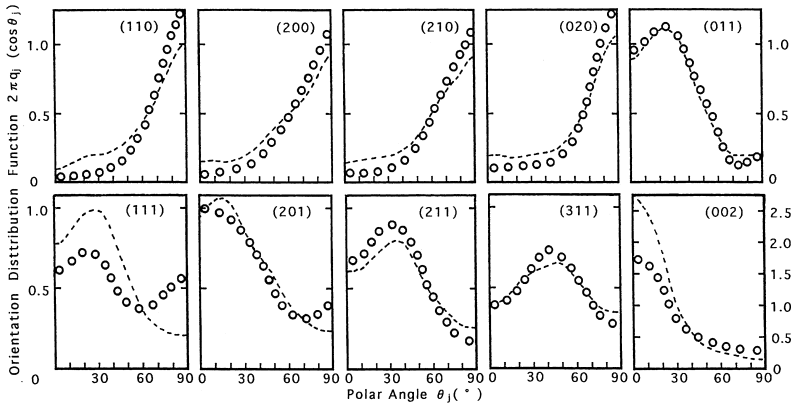

FIGURE 2 Orientation distribution functions $2\pi q_j(\cos\theta_j)$ of the reciprocal lattice vectors of the indicated crystal planes of an undrawn polyethylene film. Circles: values of $2\pi q_j(\cos\theta_j)$ obtained from experimental measurements. Dashed curves: calculated with the 21-term series. (Ref. [8]).

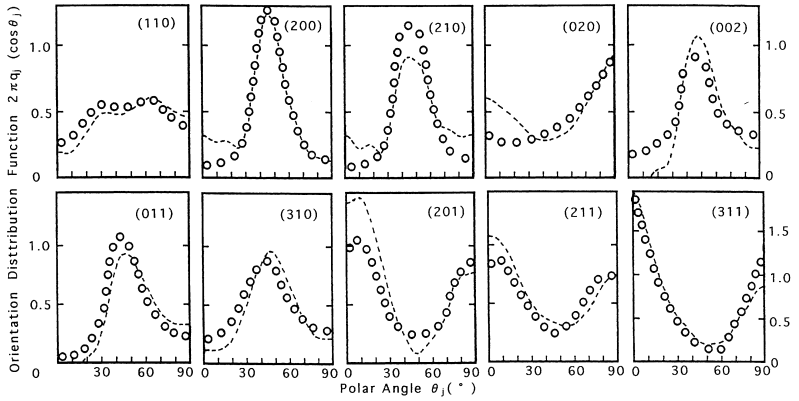

FIGURE 3 Orientation distribution functions $2\pi q_j(\cos\theta_j)$ of the reciprocal lattice vectors of the indicated crystal planes of a drawn polyethylene film with draw ratio of 2×2. Circles: values of $2\pi q_j(\cos\theta_j)$ obtained from experimental measurements. Dashed curves: calculated with the 21-term series. (Ref. [8]).

The values of R in Eq. (6) were 7.5% at $\lambda = 1$, 8.3% at $\lambda = 2 \times 2$, and 8.9% at $\lambda = 8.7 \times 8.7$.

Figures $2 \sim 4$ were listed elsewhere [8]. However, these figures are dispensable to discuss the accuracy of the generalized second and fourth

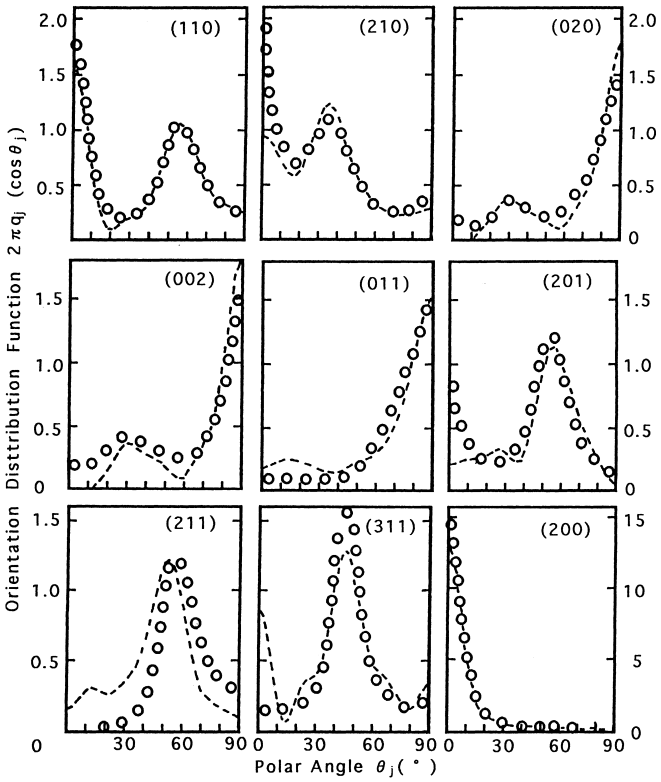

FIGURE 4 Orientation distribution functions $2\pi q_j(\cos\theta_j)$ of the reciprocal lattice vectors of the indicated crystal planes of a drawn polyethylene film with draw ratio of 8.7×8.7. Circles: values of $2\pi q_j(\cos\theta_j)$ obtained from experimental measurements. Dashed curves: calculated with the 21-term series. (Ref. [8]).

order orientation factors. It is evident that fairly good agreement between the observed and calculated distribution functions of the reciprocal lattice vectors of the indicated crystal planes was obtained, even for less accurately measured crystal planes with lower weighing factors. This indicates that the generalized second and fourth order factors needed to calculate Young's modulus could be obtained with high experimental accuracy. The orientation of crystallites was discussed on the basis of the results in Figures $2 \sim 4$ elsewhere [8] in detail.

Orientation Factors of Amorphous Chain Segments

In order to characterize the orientation behavior of crystallites within the dry gel films, the second order orientation factor of the amorphous chain segments was obtained from the birefringence as estimated by subtraction of the crystalline contribution from the total birefringence, assuming simple additivity as indicated in the following equation [16]:

$$\Delta_{total} = X_c\Delta_c + (1 - X_c)\Delta_a + \Delta_f \tag{8}$$

where Δ_{total} is the total birefringence of the bulk specimen, Δ_{c} is the crystalline birefringence, Δ_{a} is the non-crystalline birefringence, X_{c} is the volume fraction of crystalline phase, and Δ_{f} is the form birefringence. Δ_{c} and Δ_{a} are given by

$$\begin{aligned}\Delta_c &= n_a F_{200}^{[200]} + n_b F_{200}^{[020]} + n_c F_{200}^{[002]} \\ &= (n_c - n_a)F_{200}^{[002]} + (n_b - n_a)F_{200}^{[020]}\end{aligned} \tag{9}$$

and

$$\Delta_a = (n_{\parallel} - n_{\perp})F_{200}^{am} \tag{10}$$

where n_{a}, n_{b}, and n_{c} are the refractive indices along the a, b, and c-axes, which are given as 1.514, 1.519, and 1.575, respectively [17]. $\text{n}_{\parallel}$ and $\text{n}_{\perp}$ are the refractive indices parallel and perpendicular to an amorphous chain segment. The birefringence of $(\text{n}_{\parallel} - \text{n}_{\perp})$ of the amorphous chain segment is 52×10^{-3} and is the second order orientation factor. The two orientation factors, F_{20}^{j} and F_{200}^{am}, characterize the molecular orientation distribution with variation between $-1/2$ and 1. In a simultaneous biaxially stretched film, they are 0 for random orientation, while for complete orientation parallel and perpendicular to the film normal direction, they are unity and $-1/2$, respectively. In other words, when the molecular chains are perfectly oriented along the stretching direction, they become $-1/2$.

By neglecting Δ_{f}, the orientation factors of the c-axes and the amorphous chain segments may be obtained through Eq. (8)–(10). For the film with 2×2, F_{200} for crystallites and F_{200}^{am} for amorphous

chain segments are 0.0341 and -0.0779, respectively, while for the film with 8.7×8.7, F_{200} and F_{200}^{am} are -0.173 and -0.341, respectively. The preferential orientational degree of the amorphous chain segments is higher than that of the c-axes under simultaneous biaxially stretching. This indicates that the preferential orientation of the c-axes arisen by the rotation of crystallites around their b-axes to the stretching direction is due to straining of tie molecules. This process accompanies the crystal transformation from a folded to a fibrous type at initial draw ratio $< 2 \times 2$, which indicates the drastic decrease in crystallinity as described in a previous paper [8].

RESULTS AND DISCUSSION

Young's modulus of biaxially stretching film can be calculated by using the generalized orientation factors $F_{\ell 0n}$ on the basis of a two-phase model assuming the homogeneous stress hypothesis for a polycrystalline material [42, 18–21]. This treatment based on a linear elastic theory, is suitable for representing the morphology of the present simultaneous biaxially stretched films as a continuous body, since no scattering pattern was observed under Hv polarization condition associated with the existence of the aggregation of crystallites such as spherulites and rod-like textures.

Figure 5 shows the model satisfying the above concept. This model is employed as a tool to calculate the average elastic compliance in bulk and to formulate stress-strain field in bulk. Assuming that crystal unit is set in this field, the crystal strains can be represented as a function of composite mode and molecular orientation. Volume crystallinity X_c is represented by $\delta\mu^2$ by the use of the fraction lengths δ and μ in the directions of the X_3 and X_2 (and the X_1) axes. In this model system, amorphous layers are adjacent to the oriented crystalline layers with the interfaces perpendicular to the X_1, X_2 and X_3 axes. Strains of the two phases at the boundary are assumed to be identical. This model can be constructed by the following three processes. First, an anisotropic amorphous layer lies adjacent to the crystallite with the interface perpendicular to the X_3 axes and the resultant system is termed as phase I. Secondly, an anisotropic amorphous layer with fraction length $1-\mu$ is attached to the structure of phase I in a plane

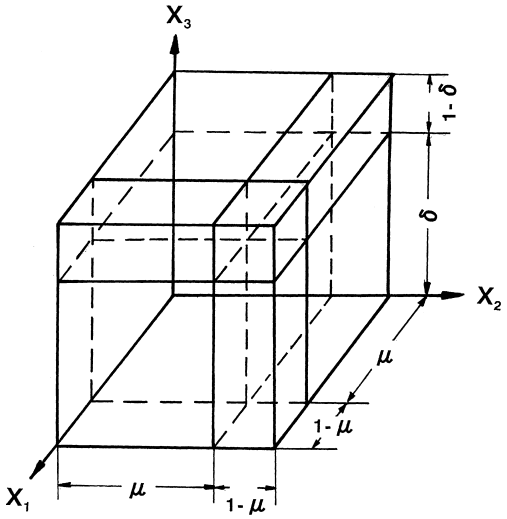

FIGURE 5 Composite model in which oriented crystallites are surrounded by an anisotropic amorphous phase.

normal to the X_1 direction to construct phase II. The final phase III can be constructed by adding an anisotropic amorphous layer with fraction length $1-\mu$ to phase II. This procedure was represented elsewhere in detail [12]. For biaxially stretched films, it is well-known that at $\mu = 1$, this model corresponds to a parallel model, while at $\delta = 1$, it corresponds to a series model. In following discussion, some representative equations are described to shorten this paper. Complicated mathematical derivation was eliminated, since such treatment is similar to that of crystal lattice modulus reported elsewhere [12, 20, 21].

In accordance with the mathematical procedure of the generalized Hook's law using the model in Figure 5, Young's modulus in the stretching direction (the X_1 and X_2 axes) can be given by [12, 20].

$$E = \frac{\mu}{S_{11}^{II}} + \frac{1-\mu}{S_{11}^{av}} + \frac{\left(S_{13}^{II}/S_{11}^{II} - S_{13}^{av}/S_{11}^{av}\right)^2}{S_{33}^{II}/\mu(1 - S_{13}^{II^2}/S_{11}^{II}S_{33}^{II}) + S_{33}^{av}/1 - \mu(1 - S_{13}^{av^2}/S_{11}^{av}S_{33}^{av})} \quad (11)$$

In Eq. (11), S_{ij}^{II} is given as a function containing S_{ij}^{I}, S_{ij}^{av} and μ. S_{ij}^{I} is also given as a function containing S_{ij}^{cv}, S_{ij}^{av} and δ in which S_{ij}^{cv}, and S_{ij}^{av} are the average compliance of crystal the amorphous phases, respectively. The complicated relationship was represented by Matsuo elsewhere [12].

The relation between the intrinsic compliance of the structural unit and the bulk compliance is given by

$$S_{ijk\ell}^{cv} = \sum_{r=1}^{3}\sum_{q=1}^{3}\sum_{p=1}^{3}\sum_{o=1}^{3}\langle a_{io}a_{jp}a_{kq}a_{\ell r}\rangle_{cv} S_{opqr}^{co} \tag{12}$$

$$S_{ijk\ell}^{av} = \sum_{r=1}^{3}\sum_{q=1}^{3}\sum_{p=1}^{3}\sum_{o=1}^{3}\langle a_{io}a_{jp}a_{kq}a_{\ell r}\rangle_{av} S_{opqr}^{ao} \tag{13}$$

where $S_{ijk\ell}^{cv}$ and $S_{ijk\ell}^{av}$ are bulk compliance of the crystal and amorphous phases, respectively, and S_{opqr}^{co} and S_{opqr}^{ao} are their intrinsic compliance. a_{io} is, for example, the direction cosine of the u_o axis with respect to the X_i axis, which is given from the geometrical arrangements in Figure 1 as follows:

$$a = \begin{vmatrix} \cos\phi\cos\theta\cos\eta - \sin\phi\sin\eta & -\cos\phi\cos\theta\sin\eta - \sin\phi\cos\eta & \cos\phi\sin\theta \\ \sin\phi\cos\theta\cos\eta + \cos\phi\sin\eta & -\sin\phi\cos\theta\sin\eta + \cos\phi\cos\eta & \sin\phi\sin\theta \\ -\sin\theta\cos\eta & \sin\theta\sin\eta & \cos\theta \end{vmatrix} \tag{14}$$

Average values of the crystal phase in Eq. (12), $\langle a_{io}\ a_{jp}\ a_{kq}\ a_{lr}\rangle_{av}$, is given by

$$\langle a_{io}a_{jp}a_{kq}a_{lr}\rangle_{av} = \int_0^{2\pi}\int_0^{2\pi}\int_0^{\pi} \omega(\theta,\eta)a_{io}a_{jp}a_{kq}a_{lr}\sin\theta d\theta d\phi d\eta \tag{15}$$

where $\omega(\theta,\eta)$ are an orientation distribution function of the crystal unit $0-U_1U_2U_3$ with respect to the coordinate $0-X_1X_2X_3$ in Figure 1. On the other hand, average values of the amorphous phase in Eq. (13), $\langle a_{io}\ a_{jp}\ a_{kq}\ a_{lr}\rangle_{av}$, is given by

$$\langle a_{io}a_{jp}a_{kq}a_{lr}\rangle_{av} = \int_0^{2\pi}\int_0^{2\pi}\int_0^{\pi} \omega_{am}(\theta)a_{io}a_{jp}a_{kq}a_{lr}\sin\theta d\theta d\phi d\eta \qquad (16)$$

where $\omega_{\mathrm{am}}(\theta)$ is an orientation distribution function of the amorphous chain segments. The treatment is somewhat complicated but realistic.

The generalized orientation factors $F_{\ell 0n}$ and $F_{\ell 00}^{am}$ of crystal and amorphous phases can be represented by using $\omega(\theta,\eta)$ and $\omega_{\mathrm{am}}(\theta)$, respectively, in the case when both the structural units have an uniaxial orientation around the X_3 axis (film thickness direction):

$$F_{\ell 0n} = \int_0^{2\pi}\int_0^{2\pi}\int_0^{\pi} \omega(\theta,\eta)P_\ell^n(\cos\theta)\cos n\eta\sin\theta d\theta d\phi d\eta \qquad (17)$$

and

$$F_{\ell 0n}^{am} = \int_0^{2\pi}\int_0^{2\pi}\int_0^{\pi} \omega_{am}(\theta)P_\ell(\cos\theta)\sin\theta\, d\theta d\phi d\eta \qquad (18)$$

The elastic compliance $S_{ijk\ell}$, represented as a tensor quantity, may be related to S_{uv} by matrix as follows:

$$\begin{array}{lllll} S_{ijk\ell} = S_{uv} & \mathrm{u} & \text{and} & \mathrm{v} \leqq 3 \\ S_{ijk\ell} = (1/2)S_{uv} & \mathrm{u} & \text{or} & \mathrm{v} \geqq 3 \\ S_{ijk\ell} = (1/4)S_{uv} & \mathrm{u} & \text{and} & \mathrm{v} \geqq 3 \end{array} \qquad (19)$$

where (ij) and (kl) become u and v, respectively. The combinations are as follows:

$$\begin{array}{lll} (1\ 1) \to 1 & (2\ 2) \to 2 & (3\ 3) \to 3 \\ (2\ 3) \to 4 & (3\ 1) \to 5 & (1\ 2) \to 6 \end{array} \qquad (20)$$

Using Eqs. (11)–(20), S_{ij}^{cv} of the crystal unit may be given by

$$\begin{aligned} S_{11}^{cv} = S_{22}^{cv} = {} & \left(\frac{1}{64}\right)S_{11}^{co}\left\{\left(\frac{1}{35}\right)F_{404} - \left(\frac{8}{35}\right)F_{402} + \left(\frac{72}{35}\right)F_{400}\right. \\ & \left. - \left(\frac{32}{7}\right)F_{202} + \left(\frac{64}{7}\right)F_{200} + \left(\frac{64}{5}\right)\right\} \\ & + \left(\frac{1}{64}\right)S_{22}^{co}\left\{\left(\frac{1}{35}\right)F_{404} + \left(\frac{8}{35}\right)F_{402}\right. \\ & \left. + \left(\frac{72}{35}\right)F_{400} + \left(\frac{32}{7}\right)F_{202} + \left(\frac{64}{7}\right)F_{200} + \frac{64}{5}\right\} \end{aligned}$$

$$
\begin{aligned}
&+ S_{33}^{co}\left\{\left(\frac{3}{35}\right)F_{400} - \left(\frac{2}{7}\right)F_{200} + \frac{1}{5}\right\} \\
&+ \left(\frac{1}{64}\right)(2S_{12}^{co} + S_{66}^{co})\left\{ - \left(\frac{1}{35}\right)F_{404} + \left(\frac{24}{35}\right)F_{400}\right. \\
&\qquad\qquad \left. + \left(\frac{64}{21}\right)F_{200} + \left(\frac{64}{15}\right)\right\} \\
&+ \left(\frac{1}{16}\right)(2S_{13}^{co} + S_{55}^{co})\left\{\left(\frac{2}{35}\right)F_{402} - \left(\frac{24}{35}\right)F_{400}\right. \\
&\qquad\qquad \left. - \left(\frac{4}{21}\right)F_{202} - \left(\frac{8}{21}\right)F_{200} + \frac{112}{105}\right\} \\
&+ \left(\frac{1}{16}\right)(2S_{23}^{co} + S_{44}^{co})\left\{ - \left(\frac{2}{35}\right)F_{402} - \left(\frac{24}{35}\right)F_{400}\right. \\
&\qquad\qquad \left. + \left(\frac{4}{21}\right)F_{202} - \left(\frac{8}{21}\right)F_{200} + \frac{112}{105}\right\}
\end{aligned}
\tag{21}
$$

$$
\begin{aligned}
S_{33}^{cv} = &\frac{1}{8}S_{11}^{co}\left\{\frac{1}{105}F_{404} - \frac{8}{105}F_{402} + \frac{24}{35}F_{400} + \frac{8}{7}F_{202} - \frac{16}{7}F_{200} + \frac{8}{5}\right\} \\
&+ \frac{1}{8}S_{22}^{co}\left\{\frac{1}{105}F_{404} + \frac{8}{105}F_{402} + \frac{24}{35}F_{400} - \frac{8}{7}F_{202} - \frac{16}{7}F_{200} + \frac{8}{5}\right\} \\
&+ S_{33}^{co}\left\{\frac{8}{35}F_{400} + \frac{4}{7}F_{200} + \frac{1}{5}\right\} \\
&- \frac{1}{8}(2S_{12}^{co} + S_{66}^{co})\left\{\frac{1}{105}F_{404} - \frac{8}{35}F_{400} + \frac{16}{21}F_{200} - \frac{8}{15}\right\} \\
&+ \frac{1}{2}(2S_{13}^{co} + S_{55}^{co})\left\{\frac{2}{105}F_{402} - \frac{8}{35}F_{400} + \frac{1}{21}F_{202} + \frac{2}{21}F_{200} + \frac{2}{15}\right\} \\
&- \frac{1}{2}(2S_{23}^{co} + S_{44}^{co})\left\{\frac{2}{105}F_{402} + \frac{8}{35}F_{400} + \frac{1}{21}F_{202} - \frac{2}{21}F_{200} - \frac{2}{15}\right\}
\end{aligned}
\tag{22}
$$

$$
\begin{aligned}
S_{12}^{cv} = &\frac{1}{64}S_{11}^{co}\left\{\frac{1}{105}F_{404} - \frac{8}{105}F_{402} + \frac{24}{35}F_{400} - \frac{32}{21}F_{202} + \frac{64}{21}F_{200} + \frac{64}{15}\right\} \\
&- \frac{1}{32}S_{12}^{co}\left\{\frac{1}{105}F_{404} - \frac{8}{35}F_{400} - \frac{320}{21}F_{200} + \frac{128}{15}\right\} \\
&+ \frac{1}{4}S_{13}^{co}\left\{\frac{1}{105}F_{402} - \frac{10}{21}F_{202} - \frac{4}{35}F_{400} - \frac{20}{21}F_{200} + \frac{16}{15}\right\}
\end{aligned}
$$

$$
\begin{aligned}
&+\frac{1}{64}S_{22}^{co}\left\{\frac{1}{105}F_{404}+\frac{8}{105}F_{402}+\frac{32}{21}F_{202}+\frac{24}{35}F_{400}+\frac{64}{21}F_{200}+\frac{64}{15}\right\}\\
&-\frac{1}{4}S_{23}^{co}\left\{\frac{1}{105}F_{402}-\frac{10}{21}F_{202}+\frac{4}{35}F_{400}+\frac{20}{21}F_{200}-\frac{16}{15}\right\}\\
&+\frac{1}{3}S_{33}^{co}\left\{\frac{3}{35}F_{400}-\frac{2}{7}F_{200}+\frac{1}{5}\right\}\\
&-\frac{1}{8}S_{44}^{co}\left\{\frac{1}{105}F_{402}+\frac{4}{21}F_{202}+\frac{4}{35}F_{400}-\frac{8}{21}F_{200}+\frac{4}{15}\right\}\\
&+\frac{1}{8}S_{55}^{co}\left\{\frac{1}{105}F_{402}+\frac{4}{21}F_{202}-\frac{4}{35}F_{400}+\frac{8}{21}F_{200}-\frac{4}{15}\right\}\\
&-\frac{1}{64}S_{66}^{co}\left\{\frac{1}{105}F_{404}-\frac{8}{35}F_{400}+\frac{128}{21}F_{200}+\frac{32}{15}\right\} \qquad (23)
\end{aligned}
$$

$$
\begin{aligned}
S_{13}^{cv}=&\frac{1}{16}S_{11}^{co}\left\{\frac{1}{105}F_{404}-\frac{8}{105}F_{402}-\frac{4}{21}F_{202}+\frac{24}{35}F_{400}+\frac{8}{21}F_{200}-\frac{16}{15}\right\}\\
&+\frac{1}{8}S_{12}^{co}\left\{\frac{1}{105}F_{404}-\frac{8}{35}F_{400}-\frac{40}{21}F_{200}+\frac{32}{15}\right\}\\
&-\frac{1}{4}S_{13}^{co}\left\{\frac{4}{105}F_{402}-\frac{5}{21}F_{202}-\frac{16}{35}F_{400}-\frac{10}{21}F_{200}-\frac{16}{15}\right\}\\
&-\frac{1}{16}S_{22}^{co}\left\{\frac{1}{105}F_{404}+\frac{8}{105}F_{402}+\frac{4}{21}F_{202}+\frac{24}{35}F_{400}+\frac{8}{21}F_{200}-\frac{16}{15}\right\}\\
&+\frac{1}{4}S_{23}^{co}\left\{\frac{4}{105}F_{402}-\frac{5}{21}F_{202}+\frac{16}{35}F_{400}+\frac{10}{21}F_{200}+\frac{16}{15}\right\}\\
&-S_{33}^{co}\left\{\frac{4}{35}F_{400}-\frac{1}{21}F_{200}-\frac{1}{15}\right\}\\
&+\frac{1}{4}S_{44}^{co}\left\{\frac{2}{105}F_{402}+\frac{1}{21}F_{202}+\frac{8}{35}F_{400}-\frac{2}{21}F_{200}-\frac{2}{15}\right\}\\
&-\frac{1}{4}S_{55}^{co}\left\{\frac{2}{105}F_{402}+\frac{1}{21}F_{202}-\frac{8}{35}F_{400}+\frac{2}{21}F_{200}+\frac{2}{15}\right\} \qquad (24)
\end{aligned}
$$

On the other hand, S_{ij}^{av} of the amorphous unit may be given by

$$
\begin{aligned}
S_{11}^{av}=S_{22}^{av}=&\left(\frac{1}{8}\right)(S_{11}^{ao}+S_{22}^{ao})\left\{\left(\frac{9}{35}\right)F_{400}^{am}+\left(\frac{8}{7}\right)F_{200}^{am}+\frac{8}{5}\right\}\\
&+S_{33}^{ao}\left\{\left(\frac{3}{35}\right)F_{400}^{am}-\left(\frac{2}{7}\right)F_{200}^{am}+\frac{1}{5}\right\}
\end{aligned}
$$

$$+\left(\frac{1}{8}\right)(2S_{12}^{ao}+S_{66}^{ao})\left\{\left(\frac{3}{35}\right)F_{400}^{am}+\left(\frac{8}{21}\right)F_{200}^{am}+\frac{8}{5}\right\}$$
$$+\left(\frac{1}{2}\right)(4S_{13}^{ao}+S_{55}^{ao}+S_{66}^{ao})\left\{-\left(\frac{3}{35}\right)F_{400}^{am}-\left(\frac{1}{21}\right)F_{200}^{am}+\frac{2}{15}\right\} \tag{25}$$

$$\begin{aligned}S_{33}^{av}=&\frac{1}{8}S_{11}^{ao}\left\{+\frac{24}{35}F_{400}+\frac{8}{5}\right\}\\&+\frac{1}{8}S_{22}^{ao}\left\{\frac{24}{35}F_{400}^{am}+\frac{8}{5}\right\}+S_{33}^{ao}\left\{\frac{8}{35}F_{400}^{am}+\frac{4}{7}F_{200}^{am}+\frac{1}{5}\right\}\\&-\frac{1}{8}(2S_{12}^{ao}+S_{66}^{ao})\left\{-\frac{8}{35}F_{400}^{am}+\frac{16}{21}F_{200}^{am}-\frac{8}{15}\right\}\\&+\frac{1}{2}(2S_{13}^{ao}+S_{55}^{ao})\left\{-\frac{8}{35}F_{400}^{am}+\frac{2}{21}F_{200}^{am}+\frac{2}{15}\right\}\\&-\frac{1}{2}(2S_{23}^{ao}+S_{44}^{ao})\left\{\frac{8}{35}F_{400}^{am}-\frac{2}{21}F_{200}^{am}-\frac{2}{15}\right\}\end{aligned} \tag{26}$$

$$\begin{aligned}S_{12}^{av}=&\frac{1}{64}S_{11}^{ao}\left\{\frac{24}{35}F_{400}^{am}+\frac{64}{21}F_{200}^{am}+\frac{64}{15}\right\}\\&-\frac{1}{32}S_{12}^{ao}\left\{-\frac{8}{35}F_{400}^{am}-\frac{320}{21}F_{200}^{am}+\frac{128}{15}\right\}\\&+\frac{1}{4}S_{13}^{ao}\left\{-\frac{4}{35}F_{400}^{am}-\frac{20}{21}F_{200}^{am}+\frac{16}{15}\right\}\\&+\frac{1}{64}S_{22}^{ao}\left\{\frac{24}{35}F_{400}^{am}+\frac{64}{21}F_{200}^{am}+\frac{64}{15}\right\}\\&-\frac{1}{4}S_{23}^{ao}\left\{\frac{4}{35}F_{400}^{am}+\frac{20}{21}F_{200}^{am}-\frac{16}{15}\right\}\\&+\frac{1}{3}S_{33}^{ao}\left\{\frac{3}{35}F_{400}^{am}-\frac{2}{7}+F_{200}^{am}+\frac{1}{5}\right\}\\&-\frac{1}{8}S_{44}^{ao}\left\{\frac{4}{35}F_{400}^{am}-\frac{8}{21}F_{200}^{am}+\frac{4}{15}\right\}\\&+\frac{1}{8}S_{55}^{ao}\left\{-\frac{4}{35}F_{400}^{am}+\frac{8}{21}F_{200}^{am}-\frac{4}{15}\right\}\\&-\frac{1}{64}S_{66}^{ao}\left\{-\frac{8}{35}F_{400}^{am}+\frac{128}{21}F_{200}^{am}+\frac{32}{15}\right\}\end{aligned} \tag{27}$$

where the generalized orientation factors may be given by

$$
\begin{aligned}
F_{200} &= \frac{1}{2}(3\langle \cos^2\theta\rangle - 1) \\
F_{202} &= 3\langle \sin^2\theta \cos 2\eta\rangle \\
F_{400} &= \frac{1}{8}(35\langle \cos^4\theta\rangle - 30\langle \cos^2\theta\rangle + 3) \\
F_{402} &= \frac{15}{2}\langle (7\cos^2\theta - 1)\sin^2\theta \cos 2\eta\rangle \\
F_{404} &= 105\langle \sin^4\theta \cos 4\eta\rangle \\
F_{200}^{am} &= \frac{1}{2}(3\langle \cos^2\theta\rangle_{am} - 1) \\
F_{400}^{am} &= \frac{1}{8}(35\langle \cos^4\theta\rangle_{am} - 30\langle \cos^2\theta\rangle_{am} + 3)
\end{aligned}
\tag{28}
$$

All the values obtained for the specimens with different draw ratios are listed in Table II. When the c-axes oriented perfectly on the film surface and the crystallinity is 100%, the Young's modulus in bulk specimen can be represented by the inverse value of S_{11}^{cv} in Eq. (21). As described in the previous paper [8], the condition can be considered as two ideal cases.; (1) the c-axes and the (200) plane are oriented perfectly parallel to the film surface. (2) the c-axes are oriented perfectly parallel to the film surface but the crystallites rotate randomly around their own c-axis. In the former case, we obtain $F_{200} = -1/2$, $F_{400} = 3/8$, $F_{202} = 3$, $F_{402} = -15/2$, and $F_{404} = 105$, while in latter case, we obtain $F_{200} = -1/2$, $F_{400} = 3/8$, $F_{202} = 0$, $F_{402} = 0$ and $F_{404} = 0$.

As discussed before (see Eq. (11)), S_{ij}^{II} is given as a function containing S_{ij}^{I}, S_{ij}^{av} and μ and S_{ij}^{I} is also given as a function of S_{ij}^{cv}, S_{ij}^{av}

TABLE II The second and fourth orientation factors of the specimens with 2×2 and 8.7×8.7

	$\lambda = 2 \times 2$	$\lambda = 8.7 \times 8.7$
F_{200}	0.0024	−0.274
F_{202}	0.463	1.6328
F_{400}	−0.204	0.166
F_{402}	3.571	−0.031
F_{404}	4.387	33.96
F_{200}^{am}	−0.0779	−0.341
F_{400}^{am}	−0.0301	0.105

and δ and consequently Young's modulus of simultaneous biaxially stretching film (X_1 and X_2 stretching directions) can be obtained using Eqs. (21)–(28).

The problem that now arises has been how the value of the intrinsic compliance S_{uv}^{co} and S_{uv}^{ao} of polyethylene can be determined theoretically. The values were initially obtained by Odajima *et al.* [22] and Tashiro *et al.* [23] using a B matrix. However, their values of S_{33}^{co} are much higher than the observed values (213–235 GPa) by X-ray diffraction [24, 25], because of the lack of inharmonic effects, indicating that their theoretical values are useful only at very low temperature close to the absolute temperature. Since then, the force fields have been improved considerably, and more recent calculations might provide much better comparison with the experimental values. For example, Lacks and Rutledge estimated the crystal lattice modulus along the chain direction as 285 GPa [26]. They calculated elastic stiffness C_{uv}^{co} except C_{44}^{co}, C_{55}^{co}, and C_{66}^{co}. Therefore, the elastic compliance S_{uv}^{ao} needed in the numerical calculation cannot be obtained by using the inverse relationship. More recent investigation by Zehnder [27] provided the best fit between the theoretical and measured values of crystal lattice modulus along the chain direction by X-ray diffraction [24, 25]. Namely, the modulus $(1/S_{33}^{co})$ calculated by using elastic compliance of a crystal unit proposed by Zehnder [27] was 216 GPa, which is very close to our experimental value in the range 213–229 GPa [25]. According to his paper [27], S_{uv}^{co} is given by

$$S_{uv}^{co} = \begin{vmatrix} 0.281 & -0.161 & -0.00036 & 0 & 0 & 0 \\ -0.172 & 0.258 & -0.0041 & 0 & 0 & 0 \\ -0.00088 & -0.0036 & 0.00462 & 0 & 0 & 0 \\ 0 & 0 & 0 & 0.474 & 0 & 0 \\ 0 & 0 & 0 & 0 & 0.599 & 0 \\ 0 & 0 & 0 & 0 & 0 & 0.431 \end{vmatrix} \times 10^{-2}/\text{GPa} \qquad (29)$$

The intrinsic elastic compliance S_{uv}^{ao} of the amorphous phase needed in the numerical calculation are not quite certain. Based on a very crude hypothesis of a biphasic structure of crystalline and non-crystalline phases, S_{uv}^{ao} can be calculated from the potential energy of neighbor chain by assuming that the following relation between the

potential energy P(r) and the atomic or molecular distance r holds for a non-crystalline chain.

$$P(r) = -\frac{c}{r^n} + \frac{d}{r^m} \tag{30}$$

where m = 9–12 and n = 1 or 6 for an ionic or molecular crystal, respectively. The elastic compliance S_{11}^{ao} and S_{22}^{ao} may be estimated by taking the second order derivative of Eq. (30).

Then,

$$S_{11}^{ao} = S_{22}^{ao} = \left(\frac{\rho_c}{\rho_a}\right)^4 S_{11}^{c'} \tag{31}$$

where $S_{11}^{c'}$ in Eq. (31) correspond to S_{11}^{cv} at $\theta = 0^0$. Thus,

$$S_{11}^{c'} = \frac{1}{8}(3S_{11}^{co} + 3S_{22}^{co} + 2S_{12}^{co} + S_{66}^{co}) \tag{32}$$

On the other hand, the expansion of the amorphous phase is assumed to occur only along the lateral direction of the polymer chain, not lengthwise. The compliance S_{33}^{ao} may be estimated by assuming that the modulus along the chain axis is proportional to the number of chain molecules in the unit area perpendicular to the chain direction, and that the modulus is independent of temperature. Thus we have

$$S_{33}^{ao} = \left(\frac{\rho_c}{\rho_a}\right) S_{33}^{co} \tag{33}$$

According to an estimation method by Hibi *et al.* [28], the other compliances can be represented as

$$\begin{aligned} S_{12}^{ao} &= -\upsilon_{21}^{ao} S_{11}^{ao} \\ S_{13}^{ao} &= S_{23}^{ao} = -\upsilon_{13}^{ao} S_{33}^{ao} \\ S_{55}^{ao} &= S_{44}^{ao} = 2(S_{11}^{ao} + \upsilon_{13}^{ao} S_{33}^{ao}) \\ S_{66}^{ao} &= 2S_{11}^{ao}(1 + \upsilon_{12}^{ao}) \end{aligned} \tag{34}$$

The Poisson ratios $\upsilon_{12}^{ao} (= \upsilon_{13}^{ao})$ is an unknown parameter and is set to be 0.47 or 0.33. The former and latter values of υ_{12}^{ao} correspond to the mechanical properties similar to the rubber elastic state and similar to tougher or glassy state, respectively.

To calculate the mechanical properties according to the previous method [29, 30] the fourth order orientation factor F_{400}^{am} of the amorphous chain segments is needed. Unfortunately, this factor cannot be obtained from birefringence measurements and therefore must be calculated by assuming a common function as an orientation function of amorphous chain segments [29, 30]. In this paper, the mean fourth power of the direction cosine $\langle \cos^4 \theta \rangle_{\mathrm{am}}$ was calculated from an inversely superposed Gaussian function G(θ) as follows [29]:

$$G(\theta) = \exp\left\{ -\frac{(\pi/2 - \theta)^2}{2\sigma^2} \right\} + \exp\left\{ -\frac{(3\pi/2 - \theta)^2}{2\sigma^2} \right\} \tag{35}$$

Using Eq. (35), the relation of $\langle \cos^4 \theta \rangle_{\mathrm{am}}$ and $\langle \cos^2 \theta \rangle_{\mathrm{am}}$ may be obtained as follows:

$$\langle \cos^n \theta \rangle_{am} = \frac{\int_0^{\pi} G(\theta) \cos^n \theta \sin \theta d\theta}{\int_0^{\pi} G(\theta) \sin \theta d\theta} \tag{36}$$

Using Eq. (36), the relation of $\langle \cos^4 \theta \rangle_{\mathrm{am}}$ and $\langle \cos^2 \theta \rangle_{\mathrm{am}}$ may be obtained. The values of $\langle \cos^4 \theta \rangle_{\mathrm{am}}$ can be obtained graphically from the experimental values of $\langle \cos^2 \theta \rangle_{\mathrm{am}}$ for amorphous chain segments, since the relation of $\langle \cos^4 \theta \rangle_{\mathrm{am}}$ and $\langle \cos^2 \theta \rangle_{\mathrm{am}}$ can be calculated by varying the parameter σ. Thus, the fourth order orientation factor F_{400}^{am} can be obtained.

Figures 6–8 show the δ-dependence of the Young's modulus E calculated at $\upsilon_{12}^{ao} (= \upsilon_{13}^{ao}) = 0.33$ and 0.47, respectively. The former and latter values of υ_{12}^{ao} correspond to the mechanical property of the amorphous phase similar to an ideal rubber elasticity and similar to somewhat tougher or glass state, respectively. The numerical calculation was carried out from Eqs. (11)–(36) using the intrinsic crystal elastic compliance S_{uv}^{co} proposed by Zehnder [27], Odajima *et al.* [22] and Tashiro *et al.* [23]. These calculated values at $\lambda = 2 \times 2$ and 8.7×8.7 are hardly affected by the Poisson's ratio of $\upsilon_{12}^{co} (= \upsilon_{13}^{ao})$ of the amorphous phases. In these figures, the relationship between δ and μ can be determined by $X_c = \delta\mu^2$ (X_c; volume crystallinity). For example, μ is 0.752 at $\delta = 1$ and 0.907 at $\delta = 0.7$ for $\lambda = 2 \times 2$ and 0.820 at $\delta = 1$ and 0.955 at $\delta = 0.7$ for $\lambda = 8.7 \times 8.7$. Interestingly, E slightly increases with μ. This tendency predicts that even for two specimens with the same crystallinity and degree of molecular orientation, their Young's

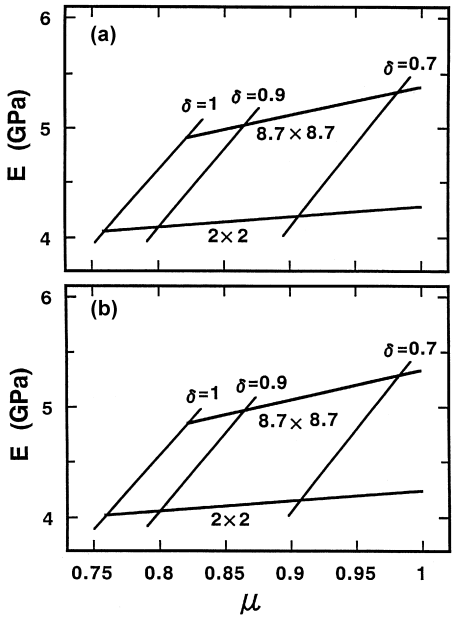

FIGURE 6 μ dependence of Young's modulus calculated by using S_{uv}^{co} of Zehnder. (a) $\upsilon_{12}^{ao}(=\upsilon_{13}^{ao}) = 0.33$, and (b) $\upsilon_{12}^{ao}(=\upsilon_{13}^{ao}) = 0.47$.

moduli slightly differ, depending on the composite mode of the crystalline and amorphous phases.

It is seen that the theoretical Young's moduli calculated at $\delta = 1$ by using S_{uv}^{co} of Zehnder [27] are in good agreement with the experimental value 4.3 GPa, at $\lambda = 8.7 \times 8.7$ as listed in Table I(b) and are in poor agreement with the experimental values, 2.2 GPa, at $\lambda = 2 \times 2$ in Table I(b). The values calculated by using S_{uv}^{co} of Odajima [22] and Tashiro *et al.* [23] deviate from the experimental results perfectly. Their large deviation is attributed to the comparison between the results measured at room temperature and the theoretical results a absolute temperature. Although the experimental values of Young's modulus (see Tabs. I(a) and (b)) are sensitive to the draw ratio, the theoretical values are less sensitive to the draw ratio as shown in Figures 6–8 in comparison with the experimental values. This is thought to be due to the fact that exact mechanical property of the simultaneous biaxially stretched PE films presented as a

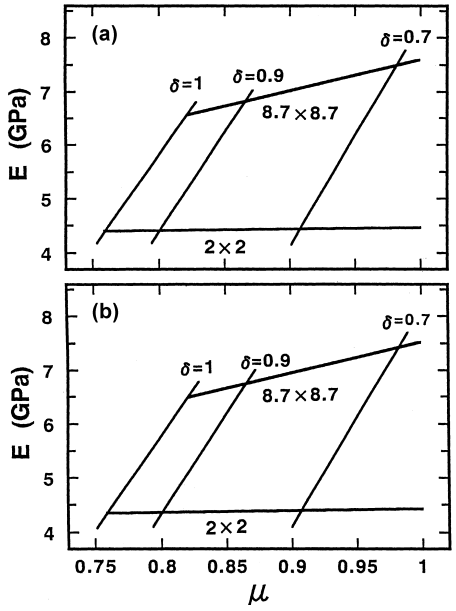

FIGURE 7 μ dependence of Young's modulus calculated by using S_{uv}^{co} of Odajima. (a) $\upsilon_{12}^{ao}(=\upsilon_{13}^{ao}) = 0.33$, and (b) $\upsilon_{12}^{ao}(=\upsilon_{13}^{ao}) = 0.47$.

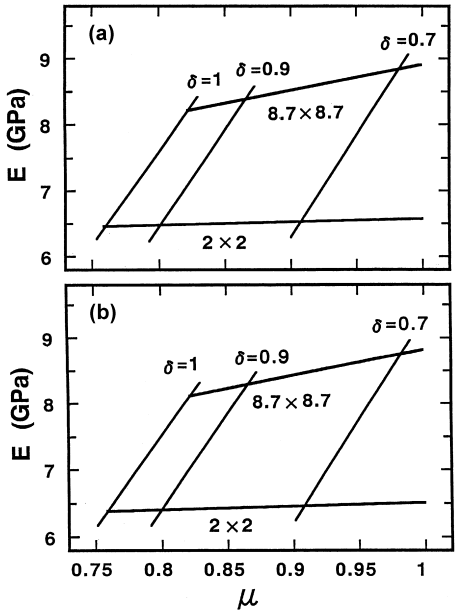

FIGURE 8 μ dependence of Young's modulus calculated by using S_{uv}^{co} of Tashiro. (a) $\upsilon_{12}^{ao}(=\upsilon_{13}^{ao}) = 0.33$, and (b) $\upsilon_{12}^{ao}(=\upsilon_{13}^{ao}) = 0.47$.

polycrystalline aggregate model cannot be represented on the homogeneous stress hypothesis by the theory for infinitesimal deformation of an anisotropic elastic body using 36 independent elastic compliance. Another possibility is due to the fact that although the elastic compliance, S_{11}^{ao} and S_{33}^{ao}, of the amorphous phase depend on the draw ratio, the values of S_{11}^{ao} and S_{33}^{ao} in Eqs. (31) and (33) are given as the intrinsic values of the amorphous phase. In addition to the above problems, furthermore consideration must be done to evaluate exact orientation distribution function of amorphous chain segment and the decreasing effect of entropy on stretching due to orientation of amorphous chains in order to achieve the good agreement between experimental and theoretical values.

CONCLUSION

Simultaneous biaxially stretching was carried out by using UHMWPE dry gel prepared by crystallization from solutions. The maximum draw ratio depended on the concentration of solutions. The greatest significant drawability could be realized at 0.9 g/100 ml with the maximum draw ratio 8.7×8.7, which is much higher than the optimum concentration of 0.45 g/100 ml assuring the draw ratio $>$ 300-fold for uniaxially stretching. The Young's modulus of the biaxially stretched film (8.7×8.7) were much lower than that of uniaxial film with almost the same draw ratio. To address the poor values of the Young's modulus, theoretical analysis was carried out by using the generalized orientation factors of crystallites and amorphous chain segments on the basis of a two phase model assuring the homogeneous stress hypothesis within a polycrystalline material. In doing so, the orientation function of crystallites was determined from the orientation of the reciprocal lattice vectors of the crystal planes using the method of Roe and Krigbaum [9–11], while the orientation function of the amorphous chain segments was assumed as an inversely superposed Gaussian function. As the intrinsic elastic compliance of a crystal unit needed to pursue the numerical calculations, three kinds of values by Zehnder [27], Odajima *et al.* [22] and Tashiro *et al.* [23] were adopted. The experimental values were in good agreement with the theoretical ones calculated by using the values of Zehnder [27]. Judging from the induced equations, the

calculated results indicated that nobody produces high modulus and high strength polyethylene sheets.

References

[1] Sakai, Y. and Miyasaka, K. (1988). *Polymer*, **29**, 1608.
[2] Sakai, Y. and Miyasaka, K. (1990). *Polymer*, **31**, 51.
[3] Sakai, Y., Uematsu, K. and Miyasaka, K. (1993). *Polymer*, **34**, 318.
[4] Gerrits, N. S. J. A., Young, R. J. and Lemsstra, P. J. (1990). *Polymer*, **31**, 231.
[5] Gerrits, N. S. J. A. and Lemsstra, P. J. (1991). *Polymer*, **32**, 1770.
[6] Gerrits, N. S. J. A. and Young, R. J. (1991). *J. Polym. Sci. Part B Polym. Phys.*, **29**, 825.
[7] Bastiaansen, C. W., Leblands, P. J. R. and Smith, P. (1990). *Macromolecules*, **23**, 2365.
[8] Nakashima, T., Xu, C., Bin, Y. and Matsuo, M. (2001). *Polymer J.*, **42**, 49.
[9] Roe, R. J. and Krigbaum, W. R. (1964). *J. Chem. Phys.*, **40**, 2608.
[10] Krigbaum, W. R. and Roe, R. J. (1964). *J. Chem. Phys.*, **41**, 737.
[11] Roe, R. J. (1965). *J. Appl. Phys.*, **36**, 2024.
[12] Matsuo, M. (1990). *Macromolecules*, **23**, 3261.
[13] Bunn, C. W. (1939). *Trans. Faraday Soc.*, **35**, 482.
[14] Matsuo, M., Inoue, K. and Abumiya, N. (1983). *Sen-i Gakkaishi*, **32**, 841.
[15] Spendly, W., Hext, G. R. and Himsworth, F. R. (1962). *Technometrics*, **4**, 441.
[16] Stein, R. S. and Norris, F. H. (1956). *J. Polym. Sci.*, **21**, 381.
[17] Hoshino, S., Powers, J., Legrand, D. G., Kawai, H. and Stein, R. S. (1962). *J. Polym. Sci.*, **58**, 185.
[18] Gupta, V. B. and Ward, I. M. J. (1967). *Macromol. Sci.*, **B1**, 373.
[19] Reuss, A. Z. (1929). *Z. Angew Math. Mech.*, **9**, 49.
[20] Hibi, S., Maeda, M., Mizuno, M., Nomura, S. and Kawai, H. (1973). *Sen-i Gakkaishi*, **29**, 137.
[21] Nomura, S., Kawabara, S., Kawai, H., Yamaguchi, Y., Fukushima, Y. A. and Takahara, H. J. (1969). *Polym. Sci.*, A-2, **7**, 325.
[22] Odajima, S. and Maeda, T. (1966). *J. Polym. Sci.*, Part C, **15**, 55.
[23] Tashiro, K., Kobayashi, M. and Tadokoro, H. (1978). *Macromolecules*, **11**, 914.
[24] Sakurada, I., Nukushina, Y. and Ito, T. (1962). *J. Polym. Sci.*, **57**, 651.
[25] Matsuo, M. and Sawatari, C. (1986). *Macromolecules*, **19**, 2036.
[26] Lacks, D. J. and Rutledge, G. C. (1994). *J. Phy. Chem.*, **98**, 1222.
[27] Zehnder, M. (1997). "Atomic Simulation of the Elasticity of Polymers", *Ph. D. Thesis* ETH-Zurich.
[28] Hibi, S., Maeda, M., Mizuno, M., Nomura, S. and Kawai, H. (1973). *Sen-i Gakkaishi*, **29**, 152.
[29] Matsuo, M., Sawatari, C., Iwai, Y. and Ozaki, F. (1990). *Macromolecules*, **23**, 32.
[30] Takahara, H., Kawai, H., Yamaguchi, Y. and Fukushima, A. (1969). *Sen-i Gakkaishi*, **25**, 60.